Using Sustainable Oil Shale Waste Powder Treated with Silane Coupling Agent for Enriching the Performance of Asphalt and Asphalt Mixture

Xuedong Guo [1], Xing Chen [1], Yingsong Li [2], Zhun Li [1] and Wei Guo [1,*]

[1] School of Transportation, Jilin University, Changchun 130022, China
[2] School of Transportation, Changchun college of architecture, Changchun 130604, China
*   Correspondence: guowei17@mails.jlu.edu.cn; Tel.: +86-153-3511-9826

check for updates

Abstract: The increase in cost of bitumen and polymer modifiers and the importance of silicon waste material management have encouraged pavement researchers to use reusable sustainable sources. Oil shale waste powder (OSP) is considered a silicon waste material, and when used in pavement prevents leaching. However, OSP, as an acidic inorganic material, has compatibility issues with asphalt, and its use with ashpalt should be considered carefully. This paper investigates the pavement performance and modification mechanism of OSP and silane coupling agent (SCA) composite modified asphalt and asphalt mixture according to conventional physical property tests: thermogravimetric analysis (TGA), fourier transform infrared spectroscopy (FTIR), differential scanning calorimetry (DSC), and a pavement performance test. The test results showed that the incorporation of OSP and SCA improved the overall properties of asphalt and asphalt mixture and the direct mixing method is more effective than the surface pretreatment method for the modification of composite modification of asphalt. Moreover, the FTIR test and DSC test indicated that the incorporation of OSP and SCA creates new chemical bonds and changes the form and quantity of the crystalline component and the transformation of components in the bitumen.

Keywords: Oil shale waste powder; Silane coupling agent; Composite modified asphalt; modification mechanism; pavement performance

1. Introduction

Asphalt has been widely used in airfield and high-grade road pavement due to its numerous advantages such as smoothness, low-vibration, high-automated construction, and easy maintenance [1–4]. Worldwide, annually, over 86 million tons of asphalt binder is combined with gravel or sand to pave roads [5–7]. However, it has been observed that the production of asphalt requires a major expenditure of natural resources, and the associated mining, refining, production, and construction produce considerable greenhouse gas emissions [8–11]. Consequently, the industry has been steadily moving towards adopting more sustainable practices [12–14].

The main objective of sustainable development is to use natural resources in the most optimized way so that, environmental and socioeconomic issues are minimized [15–17]. In the past few years, studies regarding alternative environmental friendly materials in asphalt pavement to improve its mechanical properties have been conducted [18–21]. The use of industrial waste is a promising solution to minimize environmental pollution by sinking the accumulation of waste materials, which results in a reduction of the construction costs [22,23]. Tarbay et al. presents the use of waste materials (marble and granite) and byproduct material (steel slag) as alternative to the mineral conventional filler. The test results show that all materials enhanced rutting resistance compared to the traditional

limestone filler [24]. Abo El-Naga et al. investigated the effect of using polyethylene terephthalate waste plastic materials (PTP) on improving the performance and properties of asphalt pavement. The conclusion indicated that addition of 12% of PTP increased the pavement service life 2.81 times and saved ~20% of the asphalt layer thickness [25]. Saberian et al. assessed the effect of crushed glass on the behavior of the crushed recycled materials together with crumb rubber for road pavement applications. The results indicated that the blends of waste materials, as a low-carbon concept, could be a viable and satisfactory alternative solution for future base/subbase applications [26].

Oil shale, a sedimentary rock containing organic matter, belongs to high-mineral sapropelite, a low-calorific solid fossil fuel with a light-gray to dark-brown color [27,28]. Oil shale has more than 40% ash, which is the main difference from coal. The inorganic mineral content of oil shale is approximately 50–80%, mainly including quartz, potassium feldspar, plagioclase, kaolin, clay, mica, carbonate, pyrite, etc. The oil shale resources in the world are very rich [29]. According to statistics released by the U.S. Energy Information Administration, world shale oil reserves total approximately 11 trillion to 13 trillion tons, far exceeding oil reserves. Global shale oil is generated from Cambrian to Tertiary, mainly in nine countries: United States, Congo, Brazil, Italy, Morocco, Jordan, Australia, China, and Canada. The worldwide distribution of shale oil resources is shown in Figure 1 [30].

TOP 10 COUNTRIES WITH TECHNICALLY RECOVERABLE SHALE OIL RESOURCES

RANK	COUNTRY	SHALE OIL (BILLION BARRELS)
1	RUSSIA	75
2	U.S.	58
3	CHINA	32
4	ARGENTINA	27
5	LIBYA	26
6	AUSTRALIA	18
7	VENEZUELA	13
8	MEXICO	13
9	PAKISTAN	9
10	CANADA	9
WORLD TOTAL		**345**

Figure 1. Worldwide distribution of oil shale resources.

At present, more than 90% of oil shale is used to generate electricity by combustion and refine shale oil by distillation. With the large-scale exploitation of oil shale, a large amount of waste is produced after combustion or distillation [31]. However, the majority of oil shale waste is directly piled up in the nearby waste residue field, which causes many environmental problems. Oil shale waste is a polar material that is similar to volcanic rocks and contains traces of organic residual carbon, and has a strong activity. After combustion or distillation of oil shale, the organic matter is instantaneously removed during the rapid heating process to form a porous structure. Since oil shale waste has a porous internal structure, the usage of oil shale waste is very extensive [32,33]. Hadi et al. produced low-cost, compressed, strong, lightweight masonry bricks, similarly using the oil shale ash mixed with marble and granite sludge [34]. Aljbour prepared ceramics specimens from oil shale ash and waste glass by pressing followed by heat treatment [35]. Wei et al. prepared a long-service-life asphalt mixture by drying and sieving the oil shale waste after combustion to replace the fine aggregate below 4.75 mm as required by the Open-Grade Friction Course (OGFC) [36]. Wang et al. assessed high- and low-temperature properties of asphalt pavements incorporating dry oil shale waste ash (particle size less than 0.075 mm) as partial filler. The results illustrated that the sustainable asphalt materials have better high-temperature stability and rutting resistance, and also fulfill the requirements of low-temperature cracking resistance [37].

OGFC is a high permeable mixture used as a surface coat for good friction, and splash-and-spray reduction during rain storms [38]. However, limitations of the use of such mixtures are greatly affected by the relatively low strength and low stiffness. More specifically, the pavement fails when the

asphalt binder ages and becomes brittle. Draindown—a separation of asphalt mastic from the course skeleton—can occur during storage or transport, resulting in a thin binder coating that cannot prevent particles being dislodged by traffic [39]. The thin binder film can also age more rapidly, aggravating the ravelling problem. Sometimes, this failure occurs when the pavement is only 6–8 years old; such a short life is difficult to accept [40,41]. To effectively reduce and prevent the occurrence of ravelling damages in OGFC pavements, technologies adding the modifier are effective for prolonging the OGFC pavement service life [42,43]. However, such types of modifiers have high cost, restricting their application in modifying paving asphalt. In the past few years, many studies have been conducted on alternative environmentally friendly materials in OGFC to improve its mechanical properties [44]. The use of industrial waste is a promising solution to minimize environmental pollution by sinking the accumulation of waste materials, which results in a reduction of the construction costs.

Since oil shale waste is an acidic inorganic material formed by oil shale after distillation or combustion, its compatibility with asphalt is a serious issue in the application of oil shale waste in pavement construction. However, as a new type of coupling agent, silane coupling agents contain two functional groups with different chemical properties: one is a hydrophilic fuctional group, which can be easy to react with inorganic materials, the other is an organophilic functional group, which can be easy to chemically react with an organic polymer material or to form a hydrogen bond, so that the silane coupling agent can effectively improve the compatibility of the organic material and the inorganic material, especially the acidic inorganic material. In this study, the pavement performance and modification mechanism of oil shale waste powder and silane coupling agent composite modified asphalt and asphalt mixture are systematically investigated according to conventional physical property tests: TGA test, FTIR test, DSC test, DSR test, and a pavement performance test. Moreover, the preparation method of the oil shale waste powder and silane coupling agent composite modified asphalt and the surface pretreatment method and direct mixing method are also discussed in this paper.

2. Raw Materials

2.1. Asphalt

The asphalt used in this study is Panjin 90# asphalt, which is widely used in highways, permary pavement, urban expressways, and other heavy-traffic asphalt pavement; it can also be used as raw material for emulsified asphalt, diluted asphalt, and modified asphalt. The asphalt produced by Qilu Branch of Sinopec Corp and its technical parameters are shown in Table 1.

Table 1. Technical parameters of Panjin 90# asphalt.

Technical Parameters	Penetration			15 °C Ductility	Softening Point	Wax Content	Flash Point	Solubility	Density
	15 °C	25 °C	30 °C						
Units	0.1 mm			cm	°C	%	°C	% ≥	g·cm^{-3}
Test results	31.7	86.9	142.4	>100	44.2	1.7	≥340	99.9	1.003
Test procedure	GB/T0606-2011			GB/T0605-2011	GB/T0606-2011	GB/T0615-2011	GB/T0611-2011	GB/T0607-2011	GB/T0603-2011

2.2. Oil Shale Waste Powder

Oil shale waste is an acidic inorganic material formed by oil shale after dry distillation or combustion and has the characteristics of porosity and high activity. The oil shale waste selected in this paper is the waste residue generated after the combustion of the Huadian Longteng Power Plant in Jilin Province, China, as shown in Figure 2.

Figure 2. Oil shale waste in a power plant in Jilin province China.

The color of oil shale waste is gray-brown, and the oil has a layered joint structure of shale and a large amount of flake particles. After magnifying observation, it was found that the surface of oil shale waste is rougher, the oil shale waste has a large number of micron-sized pores, and the edge of the pores is surrounded by mossy and petal-like protrusions [36]. Figure 3 shows the appearance of oil shale waste.
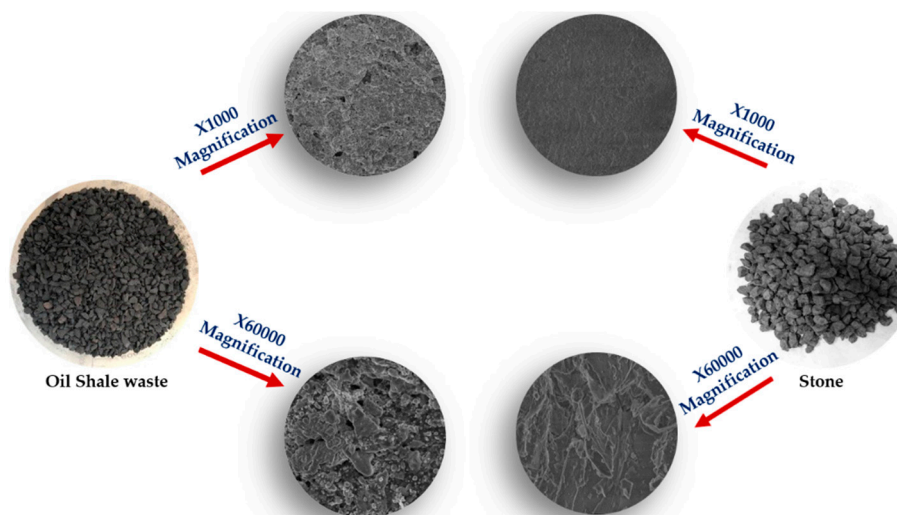

Figure 3. The appearance characteristics of oil shale waste.

The chemical composition of oil shale waste is shown in Figure 4. Figure 4 shows that the oil shale waste still retains some of the characteristics of the rock, and its main component is SiO_2, which accounts for ~53% of the total. This means that the oil shale waste can be used as a filler to reinforce bitumen. The other components are Al_2O_5, Fe_2O_3, MgO, etc., which indicates that the oil shale waste has a function. In conclusion, oil shale waste, like other silicon inorganic asphalt modifiers such as silica, diatomite, asbestos, etc., can be used for asphalt modification in terms of chemical composition. Moreover, in terms of the appearance characteristics of oil shale wastes, the porous structure can also increase the bonding between asphalt and oil shale waste.
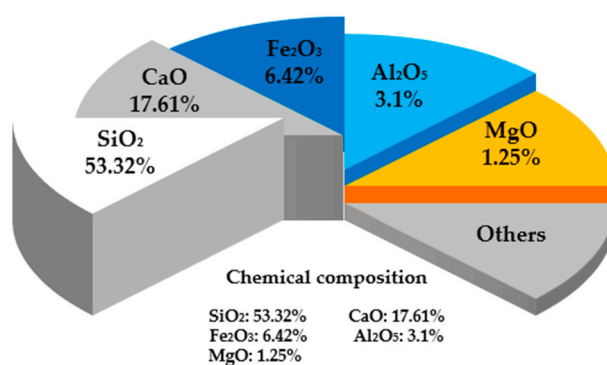
Figure 4. The chemical composition of oil shale waste

The physical properties of oil shale waste are shown in Table 2. Table 2 shows that the apparent density of the oil shale waste (OSW) is very close to that of the stone and the OSW has some characteristics of the rock. However, the OSW generated from the oil shale after extraction has higher crushing value and water absorption. The higher crushing value indicates that the residue can not bear loads as a skeleton in the asphalt mixture. Higher water absorption may lead to poor water stability of OSW in the pavement material application. In a previous study, the standard immersion Marshall test showed that utilization of oil shale waste as fine aggregate without any auxiliary modifiers reduced the water stability of asphalt mixtures, the residual stability is 70.21 % after 48 h immersion, which does not meet Chinese requirement of residual stability greater than 75% [36]. Therefore, auxiliary modifiers are needed to improve water stability during application.

Table 2. Physical parameters of OSW.

Physical Property	Apparent Density (g/cm^3)	Water Absorption (%)	Crushing Value (%)	Cohesion (Kpa)	Internal Friction Angle (°)	Optimum Water Rate (%)
OSW	2.627	18.6	42.2	13.84	33.3	28.3

It is recognized that the fineness of the inorganic asphalt modifier will determine the modification effect of the asphalt. The smaller the particle size of the modifier, the more obvious the modification effect. Therefore, oil shale waste powder with a particle size below 0.075 mm was prepared as asphalt modifier in this paper. The oil shale waste used in this paper is accumulated outdoors for a long time. Since the oil shale waste has a high moisture absorption rate, the oil shale waste should be pretreated before utilization. The pretreatment procedure of oil shale waste includes two steps of drying and smashing.

Step 1: The oil shale waste was palced in 60 °C oven for 6 h to ensure removal of moisture from the oil shale waste.

Step 2: The dried oil shale waste was immediately crushed and sieved, and oil shale waste powder with a particle size below 0.075 mm was selected as asphalt modifier.

After the oil shale waste powder was prepared, it was placed in dry box to prevent moisture intrusion. The oil shale waste powder is donoted as OSP in this paper.

2.3. Silane Coupling Agent

Silane coupling agent was first developed by Union Carbide Corp, United States. The molecular structure of the silane coupling agent includes both organic functional groups reactive with organic compounds and silane oxygen functional groups reactive with inorganic materials. Therefore, the silane coupling agent can form a stable bonding layer between the inorganic substance and the organic substance, which can effectively solve the problem of compatibility between the organic material and

the inorganic material [45]. At present, silane coupling agents have been widely used in various fields. Typical silane coupling agents are KH550, KH570, etc. Among different varieties of silane coupling agent, KH550 is mainly used in mineral-filled thermoplastic and thermosetting resins, such as polyester, epoxy, PBT, carbonate, etc., which can significantly improve and enhance the physical and mechanical properties of the material such as compressive strength, dry and wet flexural strength, shear strength, and electrical properties in the wet state. It can also be applied to the surface treatment of inorganic fillers such as silica, clay, mica, pottery clay, kaolin, etc., to enhance the wettability and dispersibility of the filler in the polymer. According to the previous research of our project team, it was found that the silane coupling agent KH550 has an obvious modification effect on acid stone. Since the oil shale waste powder is an acid stone, the silane coupling agent is finally selected as an auxiliary modifier. The auxiliary modifier silane coupling agent KH550 used in this paper is produced by Shanghai Yiyan Co., Ltd. The technical parameters of silane coupling agent KH550 are shown in Table 3.

Table 3. Technical parameters of silane coupling agent KH550.

Technical Parameters	Chromaticity	Purity	25 °C Viscosity	25 °C Density	Flash Point	Ignition Point	Boiling Point	Molecular Weight
Units	-	%	cp	g/cm^3	°C	°C	°C	1
Test results	<25	≥98.5	16	0.946	96	297	217	221.37

2.4. Aggregate

Since the surface of the alkaline aggregate is extremely active, it can obtain a stronger adhesion effect with the asphalt. In engineering, alkaline stone is generally used as the aggregate for pavement construction. The aggregate used in the paper is the limestone produced from Jiutai Stone Factory, and the technical parameters of the coarse aggregate, fine aggregate, and mineral powder are shown in Tables 4–6 according to the Chinese Test Methods of Aggregate For Highway Engineering (JTG E42-2005).

Table 4. Technical parameters of coarse aggregate

Technical Parameters		Unit	Values	Requirements	Test Procedure
Crushing value		%	21.2	≤26	T 0316-2005
Los Angeles abrasion value		%	25	≤28	T 0317-2005
Elongated particles content		%	9.3	≤15	T 0312-2005
Water absorption		%	0.61	≤2.0	T 0307-2005
Apparent specific gravity	16 mm	g·cm^{-3}	2.788		
	13.2 mm	g·cm^{-3}	2.787	≥2.6	T 0304-2005
	9.5 mm	g·cm^{-3}	2.787		
	4.75 mm	g·cm^{-3}	2.749		

Table 5. Technical parameters of fine aggregate

Technical Parameters	Unit	Values	Requirements	Test Procedure
Apparent specific gravity	g·cm^{-3}	2.71	≥2.5	T 0330-2005
Specific gravity of gross volum	g·cm^{-3}	2.64	N/A	T 0328-2005
Surface dry specific gravity	g·cm^{-3}	2.60	N/A	T 0331-1994
Mud content	%	1.02	≤3.0	T 0333-2000

Table 6. Technical parameters of mineral powder.

Technical Parameters		Unit	Values	Requirements	Test Procedure
Apparent specific gravity		$g \cdot cm^{-3}$	2.83	≥ 2.5	T 0352-2000
Water absorption		%	0.2	≤ 1	T 0353-2005
Appearance characteristic		N/A	No agglomeration	No agglomeration	N/A
Granular composition	<0.6 mm	%	100	100	
	<0.15 mm	%	98	90–100	T 0351-2000
	<0.075 mm	%	92	75–100	

3. Sample Preparation

3.1. Preparation of OSP/SCA Composite Modified Asphalt

There are two application methods of silane coupling agent for auxiliary modification: direct mixing method and surface pretreatment method. The direct mixing method is a method in which silane coupling agent stock solution is added during the mixing of inorganic material and organic filler. Generally, the silane coupling agent stock solution is first added to the organic polymer material and uniformly mixed, and then the inorganic filler is added. The surface pretreatment method involves dipping, spraying, or brushing the silane coupling agent solution on the surface of inorganic filler for surface modification.

3.1.1. Surface Pretreatment Method

Surface pretreatment method mainly consists of two steps: hydrolysis and solidification.

Step 1: Hydrolysis. Before surface modification, the silane coupling agent should be mixed with a proportion of water and ethanol solution for a period of time to achieve hydrolysis. Then, the surface of OSP is dipped with the hydrolyzed silane coupling agent solution. The silanol hydroxyl group formed by the hydrolysis reaction first forms a hydrogen bond on the surface of OSP, and then forms a coating film on the surface of OSP by dehydration reaction. During the hydrolysis reaction, the degree of hydrolysis of the silane coupling agent affects surface modification of OSP. The ratio of silane coupling agent, water, and ethanol is 5: 45: 50, and the hydrolysis time is 20 min.

Step 2: Solidfication. After the surface of OSP is treated with the silane coupling agent solution, it should also be subjected to solidfication reaction, that is, heat drying. After the solidfication reaction, part of the hydrogen bond forms a covalent bond due to dehydration, and the silane coupling agent will be in a firm or fixed state on the surface of OSP. Both the solidfication temperature and the solidfication time have an effect on the strength of the silane film. According to the previous research conclusions and actual preheating requirements of the aggregate in laboratory, the solidfication temperature is selected as 160 ° C and the solidfication time is 2 h.

In addition to the above two factors, the amount of silane coupling agent also needs to be considered in the procedure of surface modification of OSP. According to the experimental research, the surface modification effect is best when the amount of silane coupling agent solution is 2 wt% of OSP.

Since there is no currently existing literature on asphalt binders with OSP modified by SCA, at the beginning of this study, conventional tests, including penetration (ASTM D5), softening point (ASTM D36), and ductility (ASTM D113), were conducted to optimize the preparation procedure of OSP/SCA composite modified asphalt by surface pretreatment method. The test results showed that 5% OSP modified by SCA by weight of the base asphalt binder could be appropriate. Figure 5 schematically shows the preparation procedure of OSP/SCA composite modified asphalt by surface pretreatment method.
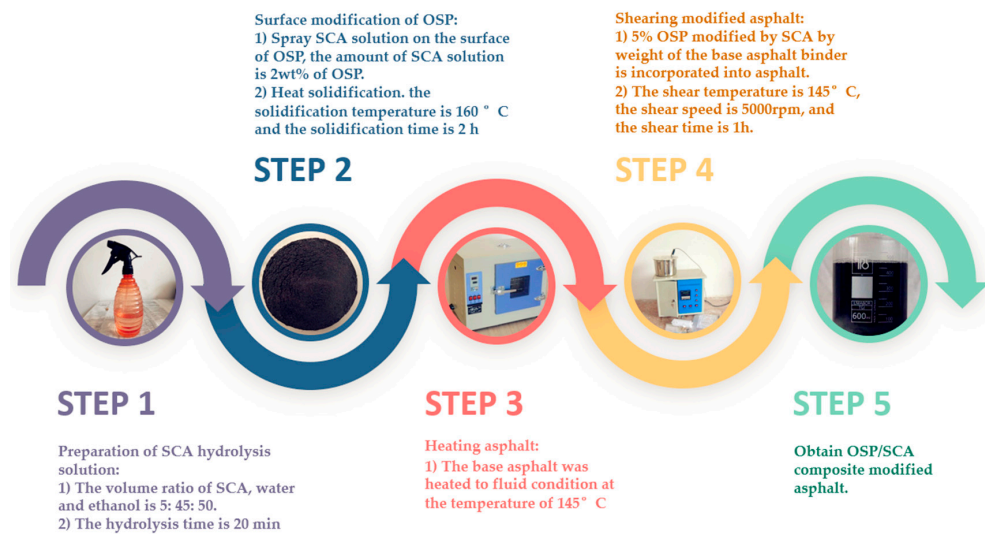
Figure 5. Preparation procedure of OSP/SCA composite modified asphalt by surface pretreatment method.

3.1.2. Direct Mixing Method

The whole preparation procedure of OSP/SCA composite modified asphalt by direct mixing method can, generally, be divided into four stages:

Step 1: The base asphalt was heated to ~135 ° C to ensure that the asphalt is completely melted and in a flowing state.

Step 2: The SCA stock solution was directly mixed into the base asphalt, and then manually stirred for 3 min.

Step 3: The OSP was mixed into the asphalt containing SCA in batches, and then manually stirred for 5 min.

Step 4: The asphalt containing SCA and OSP was immediately stirred at 5000 rpm for 1 h to evenly disperse SCA and OSP.

The amount of SCA and OSP and the shear temperature are the main factors affecting the property of OSP/SCA composite modified asphalt. The OSP/SCA composite modified asphalt with direct mixing method were prepared via similar optimization procedure. The optimization procedure is based on a orthogonal experimental design method, in which the amount of SCA is 0 wt%, 1 wt%, 2 wt%, and 3 wt% of asphalt; the amount of OSP is 0 wt%, 3 wt%, 6 wt%, and 9 wt% of asphalt; and the shear temperature is 135 °C, 145 °C, 155 °C, and 165 °C. Moreover, the evaluation indicators are penetration index, softening point, and ductility, which characterize the temperature susceptibility, high-temperature properties, and low-temperature properties of composite modified asphalt, respectively. The optimization results show 6 wt% OSP of the base asphalt binder, 2 wt% SCA of the base asphalt, and 145 °C shear temperature could be appropriate. In addition, in another set of samples, SBS modified asphalt was also prepared for comparison. The SBS modified asphalt was obtained from the Jilin Traffic Planning and Design Institute, China. For convenience, the OSP/SCA composite modified asphalt prepared by surface pretreatment method and direct mixing method are denoted as OSMA-SP and OSMA-DM, respectively. Meanwhile, base asphalt and SBS modified asphalt are denoted as BA and SMA, respectively.

3.2. Preparation of Composite Modified Asphalt Mixture

The asphalt mixture specimens modified by OSP and SCA in this paper consisted of OGFC with a nominal maximum size of 16 mm, which has been extensively applied for sustainable pavement around the world because of high skid resistance, low noise and splash-and-spray reduction. The gradation of OGFC-16 is illustrated in Figure 6.
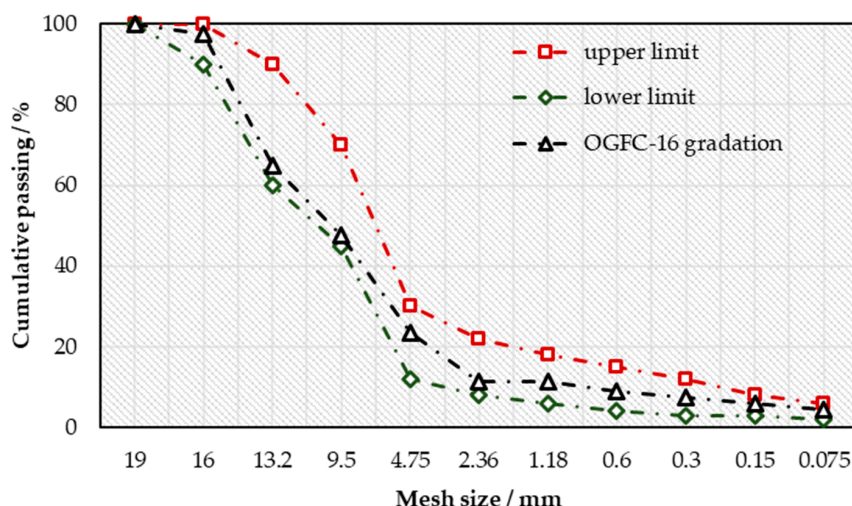
Figure 6. Gradation of OGFC-16 in the test.

　　Moreover, unmodified asphalt mixture and SBS modified asphalt mixture were prepared for comparison. The optimized bitumen–aggregate ratio of the asphalt mixture used in the study was determined by Schellenberg binder drainage test and Cantabro test. The optimized bitumen–aggregate ratio of unmodified OGFC, SBS modified OGFC, and OSP/SCA composite modified OGFC is 4.8%, 4.2%, and 4.6%, respectively. In order to simplify the sample appellation, unmodified OGFC, SBS modified OGFC, and OSP/SCA composite modified OGFC are donated as OGFC, SBS-OGFC, and OSP/SCA-OGFC, respectively, in this study.

4. Experimental Procedures

　　The detailed experimental procedures of this paper are listed in Table 7. In order to assess the property of asphalt and asphalt mixture systematically, the experimental procedures are divided into two aspects: experimental procedures of asphalt and asphalt mixture. The mechanical properties of ORF/SCA composite modified asphalt, in terms of low-temperature properties, high-temperature properties, temperature susceptibility, and anti-aging properties, were determined by three major index tests (penetration, softening point, and ductility) and the rolling thin film oven test (RTFOT). The effect of ORF and SCA on the behavior and stability properties of asphalt were determined by TGA test (Netzsch Co., Berlin, Germany). The temperature range of the test was from room temperature to 900 °C, and the heating rate was controlled at 20 °C/min. The FTIR and DSC tests were conducted to explore the modification mechanism of OSP/SCA composite modified asphalt. A Vertex 70 Fourier Transform Infrared Spectroscope (Bruker Optics Co., Changchun, China) was employed with wavelength ranging from 40 cm^{-1} to 4000 cm^{-1}. DSC tests were conducted using a DSC-500B (Shanghai yinuo precision instrument co. Ltd., China) to get the thermographs of both neat and modified asphalt binders.

　　In this section, high- and low-temperature mechanical properties, moisture-sensitive properties, raveling resistance properties, and permeability of OSP/SCA composite modified asphalt mixture were studied respectively. Specifically, the high-temperature mechanical properties of OSP/SCA composite modified asphalt mixture was evaluated by Marshall stability test and wheel tracking test. The low-temperature mechanical properties of OSP/SCA composite modified asphalt mixture was analyzed through the −15 °C splitting test and −10 °C beam-bending test. The moisture-sensitive properties of the asphalt mixture were evaluated by immersion Marshall test and self-designed spring-thawing stability test. To better evaluate the water stability of OGFC in the spring-thawing season, we use the spring-thawing stability index to evaluate the water stability of OGFC in the spring-thawing season. The specimens were treated by vacuum saturation at 97.3 kPa for 15 min and submerged in a container containing water, then the container with specimens were placed in

the precision temp-enclosure at −15 °C and frozen 12 h. Then, the specimens were soaked in water at 15 °C for 12 h through controlling the precision temp-enclosure. As described above, a complete freeze–thaw cycle is completed. After 5 freeze–thaw cycles, damaged specimens were collected for Marshall test according to Chinese standards GB/T0709-2011 [36]. The raveling resistance properties of asphalt mixture was analyzed through standard Cantabro test, and permeability was evaluated by constant head permeability test. In order to ensure the validity and repeatability of the data, the number of parallel tests in each group of experiments was 4–6.

Table 7. Experimental procedure of OSP/SCA modified asphalt and asphalt mixture.

Type	Performance	Tests	Specification	ASTM Standards
Asphalt	Physical properties	Penetration	T0604	D 5
		Softening point	T0606	D 36-00
		Ductility	T0605	D 113-99
		RTFOT	T0609	D 2872
	Thermal property	TGA	N/A	N/A
		DSC	N/A	N/A
	Modification mechanism	FTIR	N/A	N/A
Asphalt mixture	High-temperature property	Marshall stability test	T0709	D 5581-01
		Wheel tracking test	T0919	
	Low-temperature property	−15 °C splitting test	T0716	D 4123
		−10 °C beam-bending test	T0715	N/A
	Moisture-sensitive property	Immersion Marshall test	T0709	D 1075
		Spring-thawing stability test	N/A	N/A
	Raveling resistance property	Standard Cantabro test	T0733	T 305-97
	Permeability	Constant head permeability test	T0730	PS 129

5. Experimental Results and Discussion

5.1. Conventional Physical Property Test Results

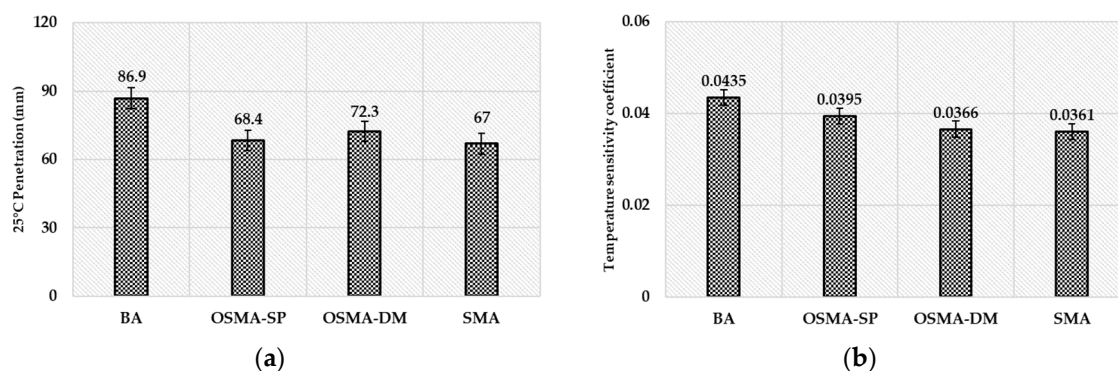The penetration test results of asphalt sample are shown in Figure 7.

Figure 7. Penetration test results of four asphalt samples: (**a**) 25 °C penetration of four asphalt samples and (**b**) temperature sensitivity coefficient of four asphalt samples.

It can be seen from Figure 7a that the incorporation of modifier reduces the penetration value of asphalt sample. This may due to the swelling and absorption reaction between the asphalt and modifier after the incorporation of modifier and mechanical stirring, which changes the structure of the asphalt colloid and enhances the gelation of the asphalt. The intercept (K) and slope (A) were obtained

to calculate penetration index (PI) through linearly regressing the logarithm of penetration (P) against temperature (T). Slope A is defined as a temperature sensitivity coefficient of asphalt. Figure 7b shows that the temperature sensitivity coefficient of asphalt is, generally, reduced after modification and the temperature sensitivity coefficient of SBS modified asphalt is the smallest. This is due to the fact that SBS, as a polymer, has a large molecular weight and viscoelastic range. The temperature sensitivity coefficient of OSP/SCA composite modified asphalt with direct mixing method is almost the same as SBS modified asphalt, and it also has excellent temperature susceptibility. This may be because OSP as a filler absorb light components with smaller molecular weight in the OSP/SCA composite modified asphalt, so that the distance between the asphalt colloid and colloid formed by OSP is reduced, and the interaction force is increased. Moreover, the bonding interaction of SCA can effectively improve the compatibility of the two components, ensuring OSP and asphalt are mixed to form a stable system. The reason why the temperature susceptibility of OSP/SCA composite modified asphalt with direct mixing method is better than surface pretreatment method may due to the large specific surface area of OSP, which is easier to agglomerate under surface pretreatment method, resulting a negative influence on the dispersion and uniformity of modified asphalt.

The softening point test results of asphalt sample are shown in Figure 8.
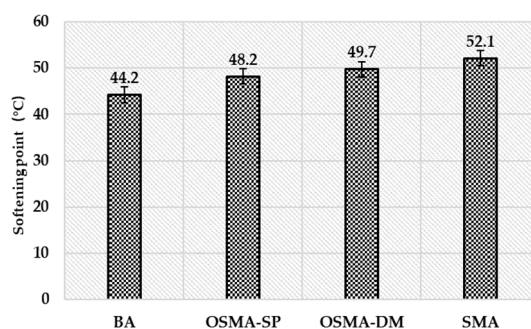

Figure 8. Softening point test results of four asphalt samples

It can be seen from Figure 8 that the softening point of modified asphalt samples is improved to different degrees compared with that of base asphalt. SBS modified asphalt, OSP/SCA composite modified asphalt with direct mixing method, and OSP/SCA composite modified asphalt with surface pretreatment method are 17.9%, 12.4%, and 9% higher than base asphalt, respectively. This indicates that both the polymer modifier and inorganic modifier can effectively improve the high temperature of asphalt. The main reason is due to the increase in the proportion of high-molecular-weight compounds and the increase of the interaction between the structures. The softening point of the composite modified asphalt is higher than that of the base asphalt partly due to the aging of the asphalt caused by long-term shearing during the preparation process.

The 10 °C ductility test results of asphalt sample are shown in Figure 9.
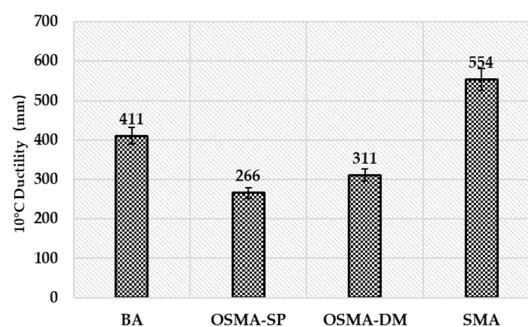

Figure 9. 10 °C ductility test results of four asphalt samples.

It can be seen from Figure 9 that the SBS modified asphalt has the largest ductility, which is beacuse SBS, as a polymer component, absorbs or adsorbs more asphalt, forming a relatively developed three-dimensional network structure in the asphalt. This three-dimensional network structure restrict the flow and sliding deformation of the asphalt molecules and improves the low temperature performance of the asphalt. Whether using the direct mixing method or surface pretreatment method, the ductility of the OSP/SCA composite modified asphalt is less than the base asphalt. This is because the temperature stress is easily concentrated at the interface of two-component at low temperature, thus the low-temperature of OSP/SCA composite modified asphalt is affected. The 10 °C ductility of OSP/SCA composite modified asphalt with surface pretreatment method is lower than direct mixing method, which is related to the a agglomerate phenomenon of OSP under surface pretreatment method.

The RTFOT aging test results of asphalt sample are shown in Table 8.

Table 8. RTFOT aging test results of four asphalt samples.

Materials	Unaged Binder			RTFO Aged Binder		
	Weight (g)	25 °C Penetration (d-mm)	10 °C Ductility (cm)	Weight (g)	25 °C Penetration (d-mm)	10 °C Ductility (cm)
BA	34.18	86.9	411	33.91	52.2	234
SMA	34.04	67	554	34.01	46.1	353
OSMA-DM	34.17	72.3	311	34.16	49.0	239
OSMA-SP	34.03	68.4	266	33.86	43.0	189

Table 8 shows that the penetration, ductility, and mass of four asphalt samples decreased after the RTFOT aging test. This loss of mass is due to the volatilization of light components after the thermo-oxidative aging of asphalt. The decrease in penetration and ductility indicates that the hardening of asphalt after RTFOT aging test, which is due to the increase of colloid and asphaltene in asphalt. The mass loss rate, 25 °C residual penetration ratio, and 10 °C residual ductility can reflect the anti-aging ability of asphalt; the smaller the mass loss rate, the greater 25 °C residual penetration ratio and 10 °C residual ductility, the better the anti-aging performance. After calculation, it is found that all the asphalt modifiers used in this paper can effectively improve the anti-aging ability of asphalt. Among them, OSMA-DM has the lowest mass loss rate and largest residual penetration ratio and residual ductility compared with the other asphalt samples, which indicates that OSMA-DM has the best anti-aging ability among the four kinds of asphalt. This is because the OSP can absorb more asphalt components to form a poly group, and the formed poly group has a thick colloidal interface layer; the long-range interaction between molecules is wide, thereby the formed structure is relatively stable. Meanwhile, the bonding interaction of SCA ensures that the adsorbed asphalt component does not precipitate from the poly group, thereby effectively enhancing the stability of the asphalt and improving the anti-aging property of the asphalt. The reason why the anti-aging property of SMA is worse than that of OSMA-DM is that SBS is a high molecular polymer. The substructure of the polymer is prone to change after thermal oxidation process, while OSP is an inorganic material that is not susceptible to thermal oxidation process.

5.2. Thermogravimetric Analysis Test Results

TGA was employed to evaluate the thermal properties of the OSP/SCA composite modified asphalt. Figure 10 presents the thermogravimetric curves of the four asphalt samples. As observed, TGA thermographs relate to particular phases of degradation with distinct initial and final degradation temperatures, and the addition of modifiers changes the distinct initial and final degradation temperatures, which is the result of pyrolysis of the specimen. The TGA of SMA is significantly different from other three kinds of asphalt, especially in the range of 400 to 500 °C, the weight loss of

SMA is faster. This may be due to the rapid cracking and volatilization of the high molecular polymer modifier between the temperature range.
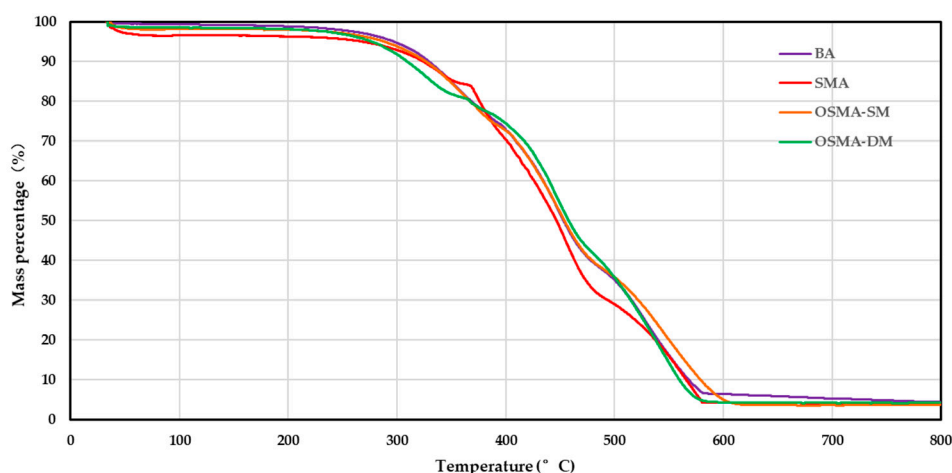

Figure 10. Thermogravimetric curves of the four asphalt samples.

From TGA curves of all the asphalt samples, the following parameters were calculated for further comprehension of the thermal properties of OSP/SCA composite modified asphalt. (1) Start of thermal degradation (temperature at 90% weight loss) (Ts, °C), (2) peak temperature (temperature at 50% weight loss) (Tp, °C), and (3) residual mass (Me, %). Table 9 present a summary of the TGA test parameters of asphalt samples.

Table 9. TGA test parameters of of four asphalt samples.

Types	Ts/°C	Tp/°C	Me/%
BA	329.2	453.0	16.1
SMA	324.0	446.5	15.9
OSMA-DM	326.4	457.7	20
OSMA-SM	309.1	453.8	14.2

As shown in Table 9, the Ts values of BA, SMA, and OSMA-DM are approximate, but the Ts value of OSMA-SP is lower than that of the other three kinds of asphalt, which indicates that the OSP with surface pretreatment of SCA is poorly dispersed in the asphalt. The Tp value of OSMA-DM was increased by 4.7 °C compared with BA, and the Me value of OSMA-DM was increased by 24% compared with BA, indicating that the high temperature stability of the asphalt is improved under the composite modification of OSP and SCA and the high temperature cracking of the asphalt is effectively suppressed. OSMA-DM has obvious improvement in Ts, Tp, and Me compared with SMA and OSMA-SP, thus indicating OSMA-DM with better thermal property, and OSP has higher dispersibility and thermal stability in OSP/SCA composite modified asphalt.

5.3. Fourier Transform Infrared Spectroscopy Test Results

Bitumen is a mixture of substances with different molecular sizes, chemical compositions, and structures. The properties of modified asphalt are determined by the nature of asphalt and modifier and the interaction between the two. At present, the modification mechanism between modifier and asphalt is generally divided into physical blending modification and chemical blending modification. The physical blending modification means that the modifier is swelled and dissolved by the action of aromatic hydrocarbons and saturated hydrocarbon, and uniformly dispersed in the asphalt to form a blend system during the preparation process. Furthermore, there is no chemical reaction and the formation of related chemical bonds during the preparation process. The chemical blending

modification refers to a chemical reaction between modifier and bitumen, which produces chemical cross-linking, chemical addition, or chemical bonds. The Fourier transform infrared spectroscopy test was employed to explore the modification mechanism of OSP/SCA composite modified asphalt. For the comprehension of FTIR spectra, the whole range is generally divided into two regions of 4000–1300 cm^{-1} and 1300–600 cm^{-1}. The peak emerged at 4000–1300 cm^{-1} is an absorption band generated by stretching vibration. Since the characteristic absorption peak of the group is usually located in this high frequency region, and the absorption peak is parsley distributed in this region, this region is the most valuable region for identifying the functional group, which is called the functional group region. In the region of 1300 to 600 cm^{-1}, in addition to the stretching vibration of single bond, there are complex spectra generated by deformation vibration. When the molecular structure is slightly different, there is a slight difference in the absorption peaks in this region. This phenomenon is like that each person has a different fingerprint, so this region is named the fingerprint region. Analysis of FTIR spectra generally requires searching for the characteristic stretching vibration of the functional group in the functional group region, and further confirming the existence of the functional group and the combination with other functional group according to the absorption peaks in the fingerprint region. The correspondence between representative chemical bonds of asphalt and FTIR spectra peak position is shown in Table 10 [46].

Table 10. Featured chemical bonds of asphalt binder.

Wave Number (cm^{-1})	Chemical Bonds
2924	The antisymmetric stretching vibration absorption band of the alkyl (C–H)
2852	The symmetric stretching vibration absorption band of the alkyl (C–H)
2729	Extensible vibration of aldehyde groups
1671	The C=O stretching vibration of primary amide carbonyl
1600	Conjugated double bonds (C=C) stretching vibration in aromatics
1456	The C–H asymmetric deformations in CH$_2$ and CH$_3$ vibrations
1377	The C–H symmetric deformation in CH$_3$ vibrations
1250	The C–O stretching vibration in saturated alcohols
1031	The sulfoxide group (S=O) stretching vibration
966	The C–H out-plane bending vibrations in unsaturated hydrocarbons
868	Benzene ring stretching vibration
747	Bending vibration of aromatic branches

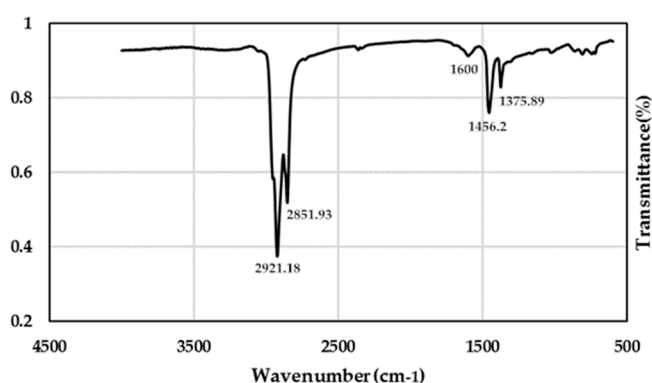The FTIR spectra of the BA, SMA, OSMA-SP, and OSMA-DM are given in Figures 11–14.
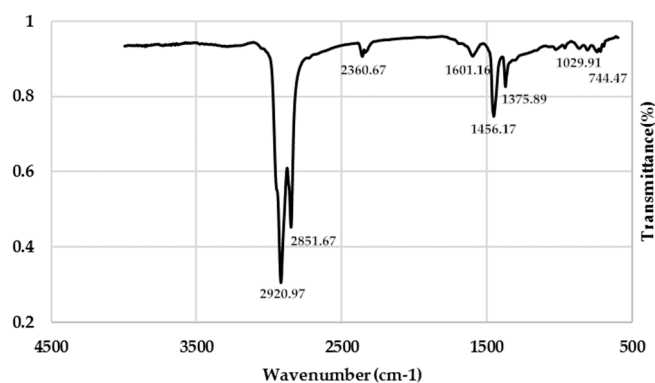

Figure 11. FTIR spectra of BA.
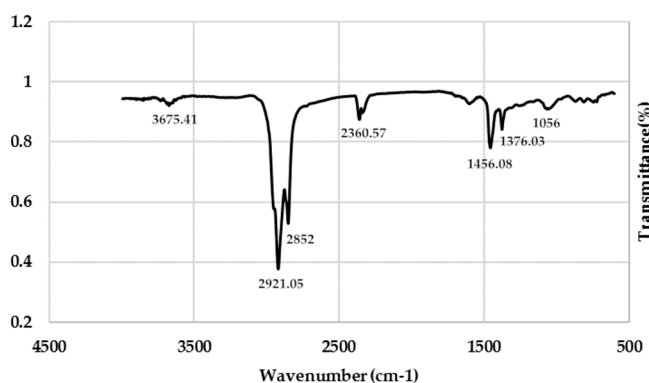
Figure 12. FTIR spectra of SMA.

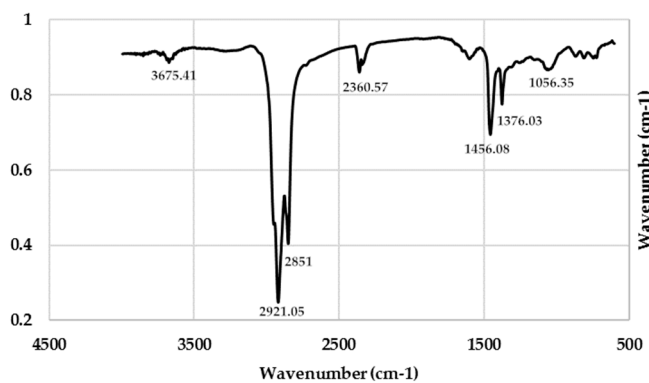**Figure 13.** FTIR spectra of OSMA-SP.

Figure 14. FTIR spectra of OSMA-DM.

From the FTIR spectrum of BA, it can be seen that the strong absorption peaks at 2918 cm^{-1} and 2851 cm^{-1} are the asymmetric and symmetric stretching vibration absorption bands of C–H in aliphatics (mainly alkanes and naphthenes), respectively, and the peak at 1600 cm^{-1} is the C–C stretching vibration in aromatics. The peaks at 1458 cm^{-1} and 1375 cm^{-1} are the in-plane bending vibration absorption peaks of C–H in aliphatics, the peak at 1032 cm^{-1} is the sulfoxide group (S=O) stretching vibration, and the four small absorption peaks in the range of 863 to 724 cm^{-1} are the out-of-plane bending vibrations of C–H on aromatic benzene rings. Thus, asphalt is mainly composed of saturated hydrocarbons, aromatics, aliphatics and heteroatom derivatives.

The FTIR spectra of SMA is similar to that of BA, it has a strong absorption peak around 2800–3000 cm^{-1} and the peak position is also basically the same as that of BA. In the functional group region, It can be seen from FTIR spectra of SMA that a absorption peak emerged at 2360.67 cm^{-1}, which may be due to the infiltration of carbon dioxide during the preparation of SMA. In the fingerprint

region, two peaks emerged at 744.47 cm^{-1} and 1029.91 cm^{-1}. The peak at 1029.91 cm^{-1} is the blending vibration of C–H in RCH=CH$_2$, indicating the RCH=CH$_2$ structure in both styrene and butadiene of SBS. Peak at 744.47 cm^{-1} is the blending vibration of aromatic branches. It can be seen that the incorporation of SBS does not change the chemical structure unit of itself and the asphalt, the modification mechanism of SMA is mainly physical blending modification.

The FTIR spectra of OSMA-SP and OSMA-DM are approximately the same. Strong absorption peaks emerged around 2800–3000 cm^{-1} are the C–H vibration of cycloalkane and alkane. Among them, the absorption peak of -CH$_2$- is the strongest, and the peaks at 2921 cm^{-1} and 2851 cm^{-1} are stretching vibration of -CH$_2$-. Different from the base asphalt, OSMA-SP and OSMA-DM have a strong absorption peak at 3675.41 cm^{-1} in the functional group region, and the peak represents an O–H vibration of the carboxyl group. This indicates that there is a new chemical bond formation in the OSMA-SP and OSMA-DM due to the graft reaction of SCA with OSP. In the fingerprint region, it was found that a new absorption peak was emerged at 1056.35 cm^{-1} in the FTIR spectra of OSMA-SP and OSMA-DM. The peak is vibration of sulfoxide group (S=O), and sulfoxide group is generally considered to be an important indicator to evaluate the aging of asphalt, which indicates that there is some thermo-oxidative aging caused by long-term shearing has occurred during the modification process of OSMA-SP and OSMA-DM..

The chemical reaction of the modifier with asphalt causes the appearance of new functional groups and the change of peak height and peak area of absorption peak. In order to quantitatively analyze the modification mechanism of three modified asphalt samples, the peak height and peak area of main functional groups of the four asphalts were statistically analyzed through ORIGIN software, as shown in Tables 11 and 12.

Table 11. The main peak area of four asphalt samples (cm).

Types	Functional Group Region				Fingerprint Region	
	3675.4 cm^{-1}	2852 cm^{-1}	2360.7 cm^{-1}	1456.2 cm^{-1}	1056.3 cm^{-1}	1029.91 cm^{-1}
BA	N/A	17.729	0.114	5.960	N/A	N/A
SMA	N/A	20.129	1.749	6.328	N/A	0.228
OSMA-SP	0.895	17.670	3.742	5.248	2.301	N/A
OSMA-DM	1.150	22.694	3.032	7.019	3.320	N/A

Table 12. The main peak height of four asphalt samples (cm).

Types	Functional Group Region				Fingerprint Region	
	3675.4 cm^{-1}	2852 cm^{-1}	2360.7 cm^{-1}	1456.2 cm^{-1}	1056.3 cm^{-1}	1029.91 cm^{-1}
BA	N/A	0.3941	0.0072	0.1603	N/A	N/A
SMA	N/A	0.4617	0.0372	0.1707	N/A	0.0082
OSMA-SP	0.0225	0.4	0.0799	0.1461	0.0311	N/A
OSMA-DM	0.0291	0.4924	0.0672	0.1991	0.0392	N/A

It can be seen from Tables 11 and 12 that the peak area and peak height of OSMA-DM are much larger than OSMA-SP at 3675.4 cm^{-1}, which indicates that more chemical bonds are generated in the OSMA-DM and SCA reacts more adequately with OSP. This conclusion is also consistent with the results of conventional physical property test. The peak height and peak area of SMA, OSMA-SP and OSMA-DM at 2360.7 cm^{-1} are much higher than that of BA. Due to the consistency of the experimental environment, only the infiltration of carbon dioxide during the preparation of modified asphalt can explain this phenomenon. The peak area and peak height of SMA and BA are slightly different at 2852 cm^{-1} and 1456.2 cm^{-1}, but the difference is not large, which indicates that the modification mechanism of SMA is mainly based on physical blending modification, but there is also certain chemical blending modification.

5.4. Differential Scanning Calorimetry Test Results

The thermal effect of asphalt during temperature change can be measured by DSC. The microscopic changes of the regate structure in asphalt can be characterized through the endothermic peak position and heat absorption of the DSC spectrum; thus, the temperature stability of asphalt can be evaluated and the modification mechanism can be speculated. The DSC spectrum of four asphalt samples are shown in Figure 15.
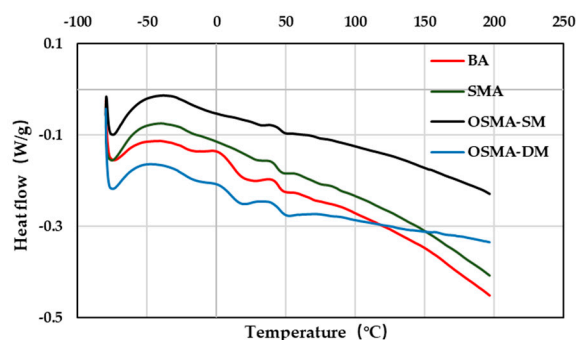

Figure 15. DSC spectrum of four asphalt samples.

As can be seen from Figure 15, the DSC spectra of the four asphalt samples are equivalent, but there are differences in some endothermic peak positions and heat absorption. The DSC curve of OSMA-DM is flatter than the other three types of asphalt, and the endothermic peak is relatively small. This indicates that the thermal stability of OSMA-DM is better than that of the other three types of asphalt, which is consistent with the conclusions of TGA test. As the temperature changes, the asphalt has three states—glassy state, viscoelastic state, and viscous flow state—and the change of state is caused by the change of regate structure with temperature. When the temperature is above 80 °C, The DSC curve of modified and unmodified asphalt has almost no endothermic peak, which indicates that most components of asphalt have completed the transition from the viscoelastic state to the viscous state at 80 °C. The DSC spectrum also indicates that the asphalt is in an endothermic or exothermic instability stage at 15 °C, 25 °C, and 30 °C, which is also the evolution process of regate structure, thus the penetration test is greatly affected with temperature under this temperature range.

The phase of asphalt changes with increasing temperature and it appears as a peak on the DSC curve. Two main parameters can be obtained on the DSC curve, one is the heat absorption during regate structure transformation, and the other is the temperature range at which regate structure transformation occurs. The endothermic peak data of modified and unmodified asphalt are summarized in Table 13.

Table 13. Endothermic peak data of four asphalt samples.

Types	Number of Peaks	Interval Heat Absorption		Total Heat Absorption (J/g)
		Temperature Range (°C)	Heat Absorption (J/g)	
BA	2	4.10 °C–41.98 °C 41.98 °C–46.92 °C	3.9782 1.9543	5.9325
SMA	1	40.34 °C–46.29 °C	1.8536	1.8536
OSMA-SM	1	41.53 °C–48.83 °C	0.9805	0.9805
OSMA-DM	2	3.19 °C–42.00 °C 42.00 °C–49.66 °C	1.9718 1.8345	3.8063

The heat absorption reflects the amount of transformed regate structure and the ratio of solid and liquid composition in the asphalt. The smaller the heat absorption, the smaller the amount of solid–liquid conversion in the asphalt and more stable the properties. Table 13 shows that the total

heat absorption of modified asphalt is reduced compared with base asphalt, which indicates that the modification process is not only a process of physical blending of two materials, but also an improvement and reinforcement of the properties of the asphalt. SCA and OSP change the large endothermic peak of base asphalt to a small endothermic peak; the DSC curve becomes relatively flat and the peak width becomes relatively narrow. This illustrates that the form and quantity of crystalline component and the transformation of components in the bitumen are changed through the incorporation of OSP and SCA. Meanwhile, the melting temperature of some components is changed, and the temperature stability and temperature susceptibility of asphalt is improved.

5.5. Pavement Performance Test Results

The pavement performance test results are shown in Table 14.

Table 14. Pavement performance test results of asphalt mixtures.

Test Item	Evolution Index	OGFC	SMA-OGFC	ORF/SCA-OGFC
Marshall stability test	Marshall stability/KN	6.47	9.12	7.26
Wheel tracking test	Dynamic stability/n/min	3340	5250	3897
−15 °C splitting test	Splitting strength/(MPa)	2.74	3.87	3.24
−10 °C beam-bending test	Bending tensile strength/(MPa) Maximum bending Strain/($\mu\varepsilon$) Bending Stiffness Modulus/(MPa)	5.202 2886 1802	7.465 4155 1796	5.920 3122 1896
Immersion Marshall test	Immersion Marshall stability/(KN)	5.73	8.21	6.4
Spring-thawing stability test	Spring-thawing stability/(KN)	5.84	8.16	6.73
Standard Cantabro test	Cantabro losses/(%)	17.4	14.2	16.8
Constant head permeability test	Permeability coefficient/(cm/s)	0.19	0.28	0.22

Table 14 shows that the high-temperature properties of the asphalt mixture are improved after the incorporation of modifier. The specification requires that the Marshall stability of OGFC should be greater than 5 KN and dynamic stability be greater than 3000 n/mm; all three asphalt mixtures meet the specifications. The Marshall stability and dynamic stability of ORF/SCA-OGFC increased by 12.2% and 16.6%, respectively, compared to OGFC, demonstrating that OSP/SCA composite modified asphalt can effectively improve the high-temperature performance of OGFC. OGFC is a skeleton structure with a large porosity. In high temperature environments, once the asphalt mortar does not provide sufficient constraints and restrictions on the skeletal structure, it will cause permanent deformation of pavement. As a kind of high viscosity modified asphalt, SBS modified asphalt can effectively increase the adhesion between asphalt and aggregate, effectively limit the relative movement between aggregates, thus, SMA-OGFC has obvious improvement in high temperature mechanical properties, especially rutting resistance. The enhancement mechanism of of high-temperature mechanical properties of SMA-OGFC and ORF/SCA-OGFC is different. The main difference is that there is a certain chemical adsorption between OSP/SCA composite modified asphalt and aggregate. The SCA in OSP/SCA composite modified asphalt has a silicon functional group and an organic group, and the silicon functional group can react with the hydroxyl group on the surface of aggregate to form a chemical bond; the organic group can react with asphalt to achieve chemical bonding, thereby the two materials of very different properties of asphalt and aggregate are "coupled" by chemical bonds, and the chemical bonding reaction is confirmed by FTIR test in the Section 5.3.

It can be seen from the −15 °C splitting test and −10 °C beam-bending test that the splitting strength and bending tensile strength of ORF/SCA-OGFC increased by 18.2% and 13.8%, respectively, compared with OGFC. This illustrates that ORF/SCA composite modified asphalt can effectively improve the low-temperature mechanical properties of OGFC. The improvement of low-temperature mechanical properties of SMA-OGFC is greater than that of ORF/SCA-OGFC. This is because OSP is an inorganic material, which is very different from the low temperature modulus of asphalt. At low

temperature, the stress is prone to generate at the interface of two-phase (OSP-asphalt) to form a shear band, which results in a relatively small improvement in low-temperature mechanical properties of ORF/SCA-OGFC.

The immersion Marshall test, spring-thawing stability test, and Cantabro Test results reveal that ORF/SCA composite modified asphalt can effectively improve the moisture damage and raveling resistance of OGFC. The immersion Marshall stability and spring-thawing stability of ORF/SCA-OGFC was 4.7% and 12.2% higher than OGFC, respectively; Cantabro losses of ORE/SCA-OGFC is 5.3% smaller than OGFC. The greater Cantabro losses indicates that the worse raveling resistance. The main reason for this is that the OSP has a special microscopic structure such as porous and large specific surface. The OSP can absorb the light weight component with less molecular weight in the asphalt, and form a series of complex interactions with asphalt, such as dispersion, superfolding, embedding, and cross-linking, which enhances the aggregate–bitumen interface bond strength and improve the mechanical structure of OGFC. Moreover, the bonding reaction of SCA at aggregate–bitumen interface is also a reason for reinforcement of mechanical properties. The permeability coefficients of OGFC, SMA-OGFC, and ORF/SCA-OGFC are 0.19 cm/s, 0.28 cm/s, and 0.22 cm/s, according to the constant head permeability test. It is well known that asphalt–aggregate ratio plays a key role in permeability performance of OGFC when the gradation is consistent. The lower the asphalt–aggregate ratio, the better the permeability performance. The permeability test results of three asphalt mixtures also confirmed this regular pattern.

In conclusion, the ORF/SCA composite modified asphalt can effectively improve the overall performance of the OGFC, although the improvement is not as good as the SBS modified asphalt, but the ORF/SCA composite modified asphalt has a strong advantage in reducing the construction cost, protecting the environment, and recycling solid waste.

5.6. Economic and Environmental Analysis

In this section, the economic and environmental analysis of SMA-OGFC and ORF/SCA-OGFC mixture in improving properties is conducted compared normal OGFC mixture. The price ratio *PR* and performance improvement ration *PIR* can be calculated by the following equation. The results are listed in Table 15.

$$PR = P_m / P_{OGFC}$$

$$PIR = PI_m / PI_{OGFC}$$

where P_m and PI_m are the price and properties of SBS-OGFC and SM-OGFC, respecitvely, and POGFC and PIOGFC are the price and properties of the normal OGFC mixture [47].

It should be noted that when referring to the marked price in China, the prices of unmodified asphalt binder, SBS and silane coupling agent are 4 CNY/kg, 15 CNY/kg and 6 CNY/kg, respectively. The average price of OGFC-16 unmodified asphalt mixture is 0.380 CNY/kg. It can be calculated that the price of graded broken stone of OGFC-16 is 0.1975 CNY/kg. At present, oil shale waste is generally deposited on open space due to no post-procedure of oil shale waste in China, so the environmental protection costs by waste accumulation cannot be accurately calculated. Therefore, the resettlement fee for construction waste is defined as the environmental protection costs of oil shale waste, and the price is ~10 CNY/kg. Since in the three asphalt mixtures only ORF/SCA-OGFC can consume oil shale waste, the environmental protection costs should be deducted for the mixture price of ORF/SCA-OGFC, and the environmental protection costs for 100 kg ORF/SCA-OGFC asphalt mixture is 2.76 CNY.

Table 15. Economic and environmental benefit analysis.

Mixture Type	Marshall Stability (kn)	Dynamic STABILITY (n/min)	−15 °C Splitting Strength (Mpa)	Bending Tensile Strength (Mpa)	Cantabro Losses (%)	Immersion Marshall Stability (kn)	Spring-Thawing Stability (kn)	Permeability Coefficient (cm/s)	Asphalt Price (CNH/kg)	Mixture Price (CNH/kg)
SMA-OGFC	9.12	5250	3.87	7.465	14.2	8.21	8.16	0.28	4.64	0.384
ORF/SCA-OGFC	7.26	3897	3.24	5.920	16.8	6.4	6.73	0.22	4.04	0.347
OGFC	6.47	3340	2.74	5.202	17.4	5.73	5.84	0.19	4.00	0.380
$PIR_{SMA-OGFC}$ and $PR_{SMA-OGFC}$	1.41	1.57	1.41	1.44	0.81	1.43	1.40	1.47	1.16	1.01
$PIR_{ORF/SCA-OGFC}$ and $PR_{ORF/SCA-OGFC}$	1.12	1.17	1.18	1.14	0.96	1.12	1.15	1.16	1.01	0.91

As shown in Table 15, the ORF/SCA composite modified asphalt improved the overall performance of the OGFC by ~10% compared with normal OGFC. Although there is a certain gap between the increase of OFR/SCA-OGFC and SBS-OGFC, the price of ORF-OGFC is lower than that of SMA-OGFC, and OFR/SCA-OGFC played an important role in reducing the cost compared with high-priced modified asphalt, especially in protecting the environment and enriching the utilization ways of oil shale waste

6. Conclusions

In this paper, the pavement performance and modification mechanism of oil shale waste powder, silane coupling agent composite modified asphalt, and asphalt mixture was systematically investigated according to conventional physical property tests: TGA test, FTIR test, DSC test, DSR test, and pavement performance test. The main conclusions are as follows.

1. The conventional physical properties test results illustrated that OSP/SCA composite modified asphalt prepared by surface pretreatment method or direct mixing method has good low-temperature properties, high-temperature properties, temperature susceptibility, and anti-aging properties. The direct mixing method is more effective than surface pretreatment method for the modification of composite modification of asphalt.
2. The TGA test results manifests that OSP/SCA composite modified asphalt has better thermal properties. Moreover, OSP/SCA composite modified asphalt with direct mixing method has better high temperature stability than surface pretreatment method, and OSP has higher dispersibility and thermal stability in composite modified asphalt.
3. The FTIR test, DSC test were carried to explore the modification mechanism of OSP/SCA composite modified asphalt. The test results indicated that the modification mechanism of OSP/SCA composite modified asphalt is not only physical blending modification but also a certain chemical blending modification. The incorporation of OSP and SCA creates new chemical bonds, and changes the form and quantity of the crystalline component and the transformation of components in the bitumen.
4. Through the pavement performance test, it was found that the OSP/SCA composite modified asphalt can effectively improve the overall performance of the OGFC. The main reason for this is that the OSP has a special microscopic structure such as porous and large specific surface. The OSP can absorb the lightweight component with less molecular weight in the asphalt, which enhances the aggregate–bitumen interface bond strength and improve the mechanical structure of OGFC. Moreover, the bonding reaction of SCA at aggregate–bitumen interface is also a reason for reinforcement of mechanical properties.

Author Contributions: Conceptualization, W.G.; Data curation, Y.S.L. and Z.L.; Formal analysis, X.C. and Z.L.; Funding acquisition, X.D.G.; Investigation, X.C.; Methodology, X.C.; Project administration, X.D.G. and W.G.; Writing—original draft, X.D.G., X.C., and Y.S.L.; Writing—review & editing, W.G.

References

1. Yuan, J.; Wang, J.Y.; Xiao, F.P.; Amirkhanian, S.; Wang, J.; Xu, Z.Z. Impacts of multiple-polymer components on high temperature performance characteristics of airfield modified binders. *Constr. Build. Mater.* **2017**, *134*, 694–702. [CrossRef]
2. Özen, H.; Aksoy, A.; Tayfur, S.; Çelik, F. Laboratory performance comparison of the elastomer-modified asphalt mixtures. *Build. Environ.* **2008**, *43*, 1270–1277. [CrossRef]
3. Pasetto, M.; Baldo, N. Unified approach to fatigue study of high performance recycled asphalt concretes. *Mater. Struct.* **2017**, *50*, 113. [CrossRef]

4. Guo, W.; Guo, X.D.; Chang, M.Y.; Dai, W.T. Evaluating the effect of hydrophobic nanosilica on the viscoelasticity property of asphalt and asphalt mixture. *Materials* **2018**, *11*, 2328. [CrossRef]

5. Rath, P.; Love, J.E.; Buttlar, W.G.; Reis, H. Performance analysis of asphalt mixtures modified with ground tire rubber modifiers and recycled materials. *Sustainability* **2019**, *11*, 1792. [CrossRef]

6. Arafat, S.; Kumar, N.; Wasiuddin, N.M.; Owhe, E.O.; Lynam, J.G. Sustainable lignin to enhance asphalt binder oxidative aging properties and mix properties. *J. Clean. Prod.* **2019**, *217*, 456–468. [CrossRef]

7. Vahidi, S.; Mogawer, W.S.; Booshehrian, A. Effects of GTR and treated GTR on asphalt binder and high-RAP mixtures materials. *J. Mater. Civ. Eng.* **2014**, *26*, 721–727. [CrossRef]

8. Swamy, A.K.; Mitchell, L.F.; Hall, S.J.; Daniel, J.S. Impact of RAP on volumetrics, stiffness, strength, and low-temperature properties of HMA. *J. Mater. Civ. Eng.* **2011**, *23*, 1490–1497. [CrossRef]

9. Fang, C.; Wu, C.; Hu, J.; Yu, R.; Zhang, Z.; Nie, L. Pavement properties of asphalt modified with packaging-waste polyethylene. *J. Vinyl Addit. Technol.* **2014**, *20*, 31–35. [CrossRef]

10. Hassana, N.A.; Airey, G.D.; Jaya, R.P.; Mashros, N.; Aziz, M.M.A. A review of crumb rubber modification in dry mixed rubberised asphalt mixtures. *J. Teknologi* **2014**, *4*, 127–134.

11. Brasileiro, L.; Moreno-Navarro, F.; Tauste-Martinez, R.; Matos, J.; Rubio-Gámez, M.D.C. Reclaimed polymers as asphalt binder modifiers for more sustainable roads: A review. *Sustainability* **2019**, *11*, 646. [CrossRef]

12. Rashad, A.M. A comprehensive overview about recycling rubber as fine aggregate replacement in traditional cementitious materials. *Int. J. Sustain. Built Environ.* **2016**, *5*, 46–82. [CrossRef]

13. Appiah, J.K.; Berko-Boateng, V.N.; Tagbor, T.A. Use of Waste Plastic Materials for Road Construction in Ghana. *Case Stud. Constr. Mater.* **2017**, *6*, 1–7. [CrossRef]

14. Chen, M.-Z.; Lin, J.-T.; Wu, S.-P.; Liu, C.-H. Utilization of recycled brick powder as alternative filler in asphalt mixture. *Constr. Build. Mater.* **2011**, *25*, 1532–1536. [CrossRef]

15. Lastra-González, P.; Calzada-Pérez, M.A.; Castro-Fresno, D.; Vega-Zamanillo, Á.; Indacoechea-Vega, I. Comparative analysis of the performance of asphalt concretes modified by dry way with polymeric waste. *Constr. Build. Mater.* **2016**, *112*, 1133–1140. [CrossRef]

16. Cao, W. Study on properties of recycled tire rubber modified asphalt mixtures using dry process. *Constr. Build. Mater.* **2016**, *21*, 1011–1015. [CrossRef]

17. Modarres, A.; Hamedi, H. Effect of waste plastic bottles on the stiffness and fatigue properties of modified asphalt mixes. *Mater. Des.* **2014**, *61*, 8–15. [CrossRef]

18. Hu, J.; Fang, C.; Zhou, S.; Jiao, L.; Zhang, M.; Wu, D. Rheological properties of packaging-waste-polyethylene-modified asphalt. *J. Vinyl Addit. Technol.* **2014**, *21*, 215–219. [CrossRef]

19. Cai, J.; Song, C.; Zhou, B.C.; Tian, Y.; Li, R.; Zhang, J.; Pei, J. Investigation on high-viscosity asphalt binder for permeable asphalt concrete with waste materials. *J. Clean. Prod.* **2019**, *228*, 40–51. [CrossRef]

20. Bowers, B.F.; Huang, B.S.; Shu, X.; Miller, B.C. Investigation of reclaimed asphalt pavement blending efficiency through GPC and FTIR. *Constr. Build. Mater.* **2014**, *50*, 517–523. [CrossRef]

21. Hosseinnezhad, S.; Kabir, S.F.; Oldham, D.; Mousavi, M.; Fini, E.H. Surface functionalization of rubber particles to reduce phase separation in rubberized asphalt for sustainable construction. *J. Clean. Prod.* **2019**, *225*, 82–89. [CrossRef]

22. Dong, Z.J.; Zhou, T.; Luan, H.; Williams, R.C.; Wang, P.; Leng, Z. Composite modification mechanism of blended bio-asphalt combining styrene-butadiene-styrene with crumb rubber: A sustainable and environmental-friendly solution for wastes. *J. Clean. Prod.* **2019**, *214*, 593–605. [CrossRef]

23. Galan, J.J.; Silva, L.M.; Perez, I.; Pasandin, A.R. Mechanical behavior of hot-mix asphalt made with recycled concrete aggregates from construction and demolition waste: A design of experiments approach. *Sustainability* **2019**, *11*, 3730. [CrossRef]

24. Tarbay, E.W.; Azam, A.M.; El-Badawy, S.M. Waste materials and by-products as mineral fillers in asphalt mixtures. *Innov. Infrastruct. Solut.* **2019**, *4*, 13. [CrossRef]

25. Abo El-Naga, I.; Ragab, M. Benefits of utilization the recycle polyethylene terephthalate waste plastic materials as a modifier to asphalt mixtures. *Constr. Build. Mater.* **2019**, *219*, 81–90. [CrossRef]

26. Saberian, M.; Li, J.; Cameron, D. Effect of crushed glass on behavior of crushed recycled pavement materials together with crumb rubber for making a clean green base and subbase. *J. Mater. Civ. Eng.* **2019**, *31*, 04019108. [CrossRef]

27. Wang, Q.; Chen, X.; Jha, A.N.; Rogers, H. Natural gas from shale formation—The evolution, evidences and challenges of shale gas revolution in United States. *Renew. Sustain. Energy Rev.* **2014**, *30*, 1–28. [CrossRef]

28. Gale, J.F.W.; Laubach, S.E.; Olson, J.E.; Eichhubl, P.; Fall, A. Natural fractures in shale: A review and new observations. *AAPG Bull.* **2014**, *98*, 2165–2216. [CrossRef]

29. Jarvie, D.M.; Hill, R.J.; Ruble, T.E.; Pollastro, R.M. Unconventional shale-gas systems: The Mississippian Barnett Shale of north-central Texas as one model for thermogenic shale-gas assessment. *AAPG Bull.* **2007**, *91*, 457–499. [CrossRef]

30. Montgomery, S.L.; Jarvie, D.M.; Bowker, K.A.; Pollastro, R.M. Mississippian Barnett Shale, Fort Worth basin, north-central texas: Gas-shale play with multi-trillion cubic foot potential. *AAPG Bull.* **2005**, *89*, 155–175. [CrossRef]

31. Bowker, K.A. Barnett Shale gas production, Fort Worth Basin: Issues and discussion. *AAPG Bull.* **2007**, *91*, 523–533. [CrossRef]

32. Vohla, C.; Koiv, M.; Bavor, H.J.; Chazarenc, F.; Mander, Ü. Filter materials for phosphorus removal from wastewater in treatment wetlands—A review. *Ecol. Eng.* **2011**, *37*, 70–89. [CrossRef]

33. Al-Qodah, Z. Adsorption of dyes using shale oil ash. *Water Res.* **2000**, *34*, 4295–4303. [CrossRef]

34. Hadi, N.A.R.A.; Abdelhadi, M. Characterization and utilization of oil shale ash mixed with granitic and marble wastes to produce lightweight bricks. *Oil Shale* **2018**, *35*, 56–69. [CrossRef]

35. Aljbour, S.H. Production of ceramics from waste glass and jordanian oil shale ash. *Oil Shale* **2016**, *33*, 260–271. [CrossRef]

36. Guo, W.; Guo, X.D.; Chen, X.; Dai, W.T. Properties analysis of oil shale waste as partial aggregate replacement in open grade friction course. *Appl. Sci.* **2018**, *8*, 1626. [CrossRef]

37. Cheng, Y.C.; Wang, W.S.; Tan, G.J.; Shi, C.L. Assessing high- and low-temperature properties of asphalt pavements incorporating waste oil shale as an alternative material in Jilin Province, China. *Sustainability* **2018**, *10*, 2179. [CrossRef]

38. Punith, V.S.; Suresha, S.N.; Raju, S.; Bose, S.; Veeraragavan, A. Laboratory investigation of open-graded friction-course mixtures containing polymers and cellulose fibers. *J. Trans. Eng.* **2012**, *138*, 67–74. [CrossRef]

39. Alvarez, A.E.; Martin, A.E.; Estakhri, C. A review of mix design and evaluation research for permeable friction course mixtures. *Constr. Build. Mater.* **2011**, *25*, 1159–1166. [CrossRef]

40. Hassan, H.F.; Al-Oraimi, S.; Taha, R. Evaluation of open-graded friction course mixtures containing cellulose fibers and styrene butadiene rubber polymer. *J. Mater. Civ. Eng.* **2015**, *17*, 416–422. [CrossRef]

41. Onyango, M.; Woods, M. Analysis of the Utilization of Open-Graded Friction Course (OGFC) in the United States. In Proceedings of the International Conference on Highway Pavements and Airfield Technology, Philadelphia, PA, USA, 27–30 August 2017.

42. Luo, S.; Qian, Z.D.; Xue, Y.C. Performance evaluation of open-graded epoxy asphalt concrete with two nominal maximum aggregate sizes. *J. Cent. South Univ. (Engl. Ed.)* **2015**, *22*, 4483–4489. [CrossRef]

43. Yang, B.; Xiong, B.; Ji, Y.; Ban, G. Experimental study of the fatigue performance of open-graded asphalt mixture friction course. *Mater. Res. Innov.* **2015**, *19*, 464–468. [CrossRef]

44. Fang, F.T.; Chong, Y.C.; Nyunt, T.T.; Loi, S.S. Development of environmentally sustainable pavement mix. *Int. J. Pavement Res. Technol.* **2013**, *6*, 440–446.

45. Xie, Y.J.; Hill, C.A.S.; Xiao, Z.F. Silane coupling agents used for natural fiber/polymer composites: A review. *Compos. Part A* **2010**, *41*, 806–819. [CrossRef]

46. Zhang, P.; Guo, Q.L.; Tao, J.; Ma, D.; Wang, Y. Aging mechanism of a diatomite-modified asphalt binder using fourier-transform infrared (FTIR) spectroscopy analysis. *Materials* **2019**, *12*, 988. [CrossRef]

47. Cai, L.C.; Shi, X.G.; Xue, J. Laboratory evaluation of composed modified asphalt binder and mixture containing nano-silica/rock asphalt/SBS. *Constr. Build. Mater.* **2018**, *172*, 204–211. [CrossRef]